

# SIMULATION OF ECCD SUPPRESSION OF NEOCLASSICAL TEARING MODES IN SAWTEETHING DISCHARGES USING 3D NONLINEAR CODE NFTC.

A.M.Popov <sup>†</sup> , R.J.La Haye <sup>‡</sup>

<sup>†</sup> Moscow State University , Moscow , Russia

<sup>‡</sup> General Atomics , San Diego , California , USA

## 1. Introduction

Nonlinear self-consistent MHD stability simulations of neoclassical tearing modes (NTM) in sawteething discharges in DIII-D tokamak are investigated using the nonlinear three-dimensional magnetohydrodynamic (MHD) code NFTC [1]. The behavior of m/n=3/2 NTMs have been observed and studied in detail in [2]. Recent experiments [3] in DIII-D demonstrate the effectiveness of NTM suppression by the radially localized electron cyclotron current drive (ECCD). Nevertheless ECCD suppression of NTM in sawteething discharges on DIII-D show difficulty in suppression when q=1 sawteeth precursors are coupled to m/n=3/2 NTM. Simulations are directed to the understanding of the mechanism of 3/2 and 1/1 mode coupling during sawtooth precursors and sawtooth crash periods and to the finding of the optimal conditions for ECCD island suppression. Required parameters of ECCD are determined for NTM suppression. The effect of differential rotation on de-coupling of 3/2 NTM and n=1 instability in precursor period is considered. The dependence of the differential rotation effect from the ratio of shears on rational surfaces m/n=3/2 and m/n=1/1 is also discussed.

## 2. Basic equations in the NFTC model

The nonlinear 3D evolution of a tokamak plasma is described by the full non-reduced, compressible, MHD system of equations which include viscosity, resistivity and sources. The equations are formulated in general toroidal geometry. The plasma can have steady-state rotation in both toroidal and poloidal directions. A model with fixed boundary conditions is used. We seek the solution  $\mathbf{Y} = \{\mathbf{V}, \mathbf{B}, \mathbf{P}\}$  of the full MHD equations, with the velocity  $\mathbf{V}$ , magnetic field  $\mathbf{B}$ , and pressure  $P$ . The functions  $\mathbf{B}_{eq}(\rho, \theta)$  and  $P_{eq}(\rho, \theta)$  describe the initial axisymmetric solution of the equilibrium equations. An arbitrary function  $\mathbf{V}_{eq}(\rho, \theta)$  describes the initial plasma rotation velocity.

The basic equations then take the following form:

$$\bar{\rho} \frac{\partial \mathbf{V}}{\partial t} = -\bar{\rho}(\mathbf{V} \cdot \nabla) \mathbf{V} - \nabla P + [(\nabla \times \mathbf{B}) \times \mathbf{B}] + \nu \nabla^2 \mathbf{V} \quad (1)$$

$$\frac{\partial \mathbf{B}}{\partial t} = [\nabla \times (\mathbf{V} \times \mathbf{B})] - [\nabla \times (\eta(\nabla \times \mathbf{B}))] + [\nabla \times \mathbf{E}_s]; \quad (2)$$

$$\frac{\partial P}{\partial t} = -\nabla \cdot (P \mathbf{V}) - (\Gamma - 1)[P(\nabla \cdot (\mathbf{V}))] + \nabla_{\parallel} \cdot (K_{\parallel} \nabla_{\parallel} P) + \nabla_{\perp} \cdot (K_{\perp} \nabla_{\perp} P) + Q; \quad (3)$$

and an equation of state which is taken to be adiabatic  $\frac{d}{dt}(\frac{P}{\bar{\rho}}) = 0$  with  $\Gamma = C_p/C_v$  the ratio of specific heats. Note that in these equations, density  $\bar{\rho}$  is assumed to be constant (unity). In these dynamic equations  $K_\perp, K_\parallel, \eta, \nu$  and  $Q$  are dimensionless values of the perpendicular thermal conductivity, finite heat conductivity along perturbed magnetic surfaces, resistivity, the kinematic viscosity and heat source term. The following are the sources of current density: the bootstrap current  $j_{BS}$ , the ECCD current  $j_{cd}$ , the current from neutral beam injection  $j_{NB}$ , the polarization current  $j_{pol}$ , the Ohmic current density  $j_\Omega$ . The total parallel current density is the sum of Ohmic current and the non-inductive current:  $j = j_\Omega + j_{BS} + j_{pol} + j_{cd} + j_{NB}$ . Then  $E = \eta j_\Omega = \eta j - E_s$ , where the source term is included as  $E_s = \eta(j_{BS} + j_{pol} + j_{cd} + j_{NB})$ . The bootstrap current  $j_{BS}$  is included in the simplest model form:  $j_{BS} = A_g \cdot 1.46 \sqrt{\varepsilon} [-\frac{\partial P / \partial \rho}{B_{pol}}]$ . The polarization current  $\tilde{j}_{pol}$  is included in the model form:  $\tilde{j}_{pol} = -\frac{W_{th}^2}{W^2} \tilde{j}_{BS}$ . In neoclassical theory the parameters  $W_{th}$  and  $A_g$  are determined by kinetic effects [4] and for MHD simulations they are the free parameters of the model. Current density  $j_{cd}$  is represented as a radially localized toroidal current of perturbed helical magnetic flux. In NFTC code we use the following simplified form

$$j_{cd} = I_{cd}(t \| W) \frac{1}{2\pi^{3/2} W_{cd}} \{ e^{-(\rho - \rho_0)/W_{cd}^2} \cdot (1 + \frac{1}{8} (\frac{W_{mn}}{W_{cd}})^2 \cos(m\theta - n\varphi + \alpha\pi)) \} \quad (4)$$

Here  $W_{mn}$  is the magnetic island width.

Metric elements  $g_{ik}(\rho, \theta)$  are calculated corresponding to the straight field line coordinate system  $\rho, \theta, \varphi$  using  $(\mathbf{B}_{eq}, P_{eq})$ , where  $\rho = \sqrt{\psi_N}$  is a radial-like coordinate which labels the magnetic surface,  $\theta$  is a poloidal-like angle, and  $\varphi$  is the toroidal angle. The numerical solution is represented as finite Fourier series in both poloidal and toroidal angles.

### 3. Suppression of the m/n=3/2 NTM in the sawtooth period

The basic equilibrium used in stability calculations is reconstructed by EFIT code for discharge # 86144.2250. In the time period of 3/2 NTM suppression in sawteething discharge there are several sawtooth periods. During this period  $q_0$  varies between greater than one and less than one. The  $q=1$  surface enters the plasma volume when 3/2 NTM has different amplitude. In period when  $q_0 > 1$ , Icd suppression is effective and when  $q_0 < 1$  the effectiveness is reduced. To compare different cases and simulate full time period of suppression we carried out the set of calculations with fitted parameters of the runs. Fig.1 shows the comparison of the full time evolution of the magnetic island width  $W_{3/2}(t)$  in discharge with no sawtooth (curve 1 and 2) and sawteething discharge (curve 3 and 4) for two different magnitudes of ECCD current: 1)  $I_{cd}/I_p = 0.033$ , 2)  $I_{cd}/I_p = 0.05$ . It is seen how the periods of suppression alternate when  $q_0 > 1$  and  $q_0 < 1$ . Also note that the increasing of the magnitude of Icd leads to suppression even in the presence of sawtooth oscillations. Fig.2 shows the comparison of effectiveness of ECCD suppression in discharge with no sawtooth  $q_{min} > 1$  and in sawteething discharge. The ratio of initial island width (when Icd was turned on) to suppressed island width  $W_s/W$  is shown versus  $I_{cd}/I_p$ . We can conclude that the magnitude of Icd should be 2-3 times more in a sawteething discharge than in discharge with no sawtooth to have the same effect of suppression. Calculations show that the coupling of the n=1 and n=2 modes can lead to reduction of effectiveness of ECCD suppression of 3/2 NTM in sawteething discharge. We study the effect of differential rotation on n=1 and n=2 modes de-coupling. Typically, the  $q=1$  fluid rotation is faster than that at  $q=3/2$ . In some of DIII-D shots such as 104232 the torques between modes keep twice the 1/1 rotation, i.e. the 2/2 rotation, at exactly the 3/2 rotation. This is where there is reduced success in ECCD suppression of

the 3/2 NTM. We choose the piece-wise plasma rotation profile in calculations. This profile permits us to change the ratio of frequencies  $\omega_2$  and  $\omega_1$  on the rational surfaces  $q=3/2$  and  $q=1$  :  $r_t = \frac{\omega_2}{\omega_1}$ , We conserve the integral under rotation profile that corresponds to comparison of discharges with the same given toroidal momentum. Fig.3a shows the effect of differential rotation in the 3/2 and 2/2 modes de-coupling . Curve 1 in figure presents the ratio of magnetic islands width  $\frac{W_{3/2}}{W_{2/2}}$  depending on the ratio  $r_t$ . The effectiveness of ECCD suppression of  $W_{3/2}$  increase with parameter  $r_t$ . There exists a ratio of frequencies where there is the most strong coupling and less suppression . When the rotation profile becomes more broad or more narrow, de-coupling increases. For chosen  $q_0 = 0.985$  and  $q$ -profile this dependence is not so strong. The effect of rotation de-coupling depends on  $q$ -profile and namely on ratio of magnetic shears on both rational surfaces. Curve 2 in fig.3a shows the same ratio of magnetic islands width depending on the ratio of magnetic shears  $S_1/S_2$ . Parameter  $5 \cdot S_1/S_2$  is shown on the x-axis to have the curve 2 on the same figure. It is seen the strong influence of this parameter in modes de-coupling. The closer the magnitudes of the magnetic shears, the more connectivity of the modes. The coupling is increased with this ratio. The more magnetic coupling of the modes the more noticeable the effect of the de-coupling due to differential rotation. Interaction of harmonics during nonlinear evolution can be seen on the time evolution of the 3/2 mode profile. Fig.3b shows the time evolution of pressure perturbation radial profiles of the  $m/n=3/2$  harmonic perturbation. ECCD is applied in this case. It is seen that although the magnetic field perturbation remains approximately the same on the rational surface  $q=3/2$  (due to Icd effect), there is the fast growing and broadening of perturbation between surfaces leading to modes coupling in the sawtooth crash. Fig.4(a,b) shows the 2D and 3D futures of 3/2 NTM ECCD suppression in sawtooth discharge : a) Poincare map of magnetic field lines when  $q_0 = 0.985$  in the presence of differential rotation in the earlier stage; b) Contour plot of pressure perturbation in the presence of differential rotation.

#### 4. Conclusions.

Self-consistent calculations using the NFTC code show the effectiveness of ECCD suppression of neoclassically destabilized magnetic islands when  $q_{min} > 1$ . In coupled sawteething discharges effectiveness of ECCD suppression of 3/2 NTM is reduced approximately by two-three times. The instability of the  $n=1$  mode shows two different scales. Instability of  $n=1$  mode with low growth rate lasts milliseconds ( what we call precursor period) and fast instability of the resistive kink mode which lasts during sawtooth crash period. The connection of 3/2 NTM with  $n=1$  (harmonics 1/1 and 2/2) instability in precursor period explain the lost of effectiveness of ECCD suppression. Differential rotation has the effect on de-coupling of 3/2 NTM and  $n=1$  instability in precursor period. The effect of differential rotation increases with the ratio of shears on rational surfaces  $m/n=3/2$  and  $m/n=1/1$ .

#### References

- [1 ]A.M.Popov,et al. Physics of Plasmas.(2001).
- [2 ]R.J.La Haye et al.,Phys.Plasmas,August 2000.
- [3 ]J.S.Degrassie,The DIII-D Team. Bull.APS, vol.45,No 7,October 2000, p219.
- [4 ]H.R.Wilson,et al.Phys.Plasmas, V.3,No.1, January 1996,p.249.

Work supported in part by U.S. DOE Grant DE-FG03-95ER54309 and Contract No. DE-AC03-99ER54463.

Effect of ECCD suppression during NTM evolution.

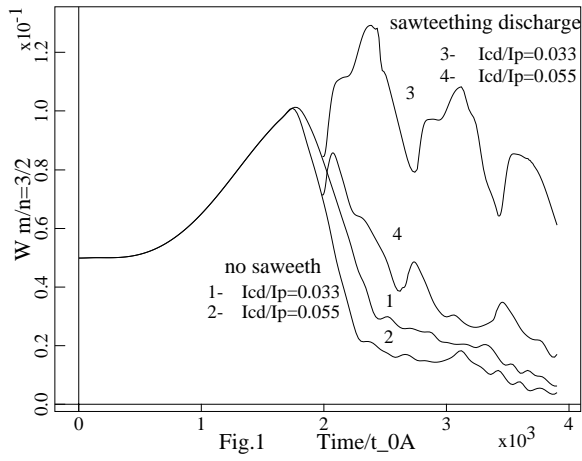


Fig.1

Effectiveness of ECCD suppression.

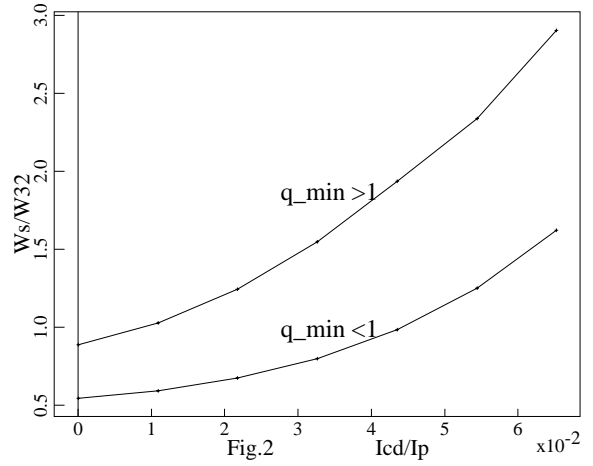


Fig.2

Differential rotation during ECCD suppression.

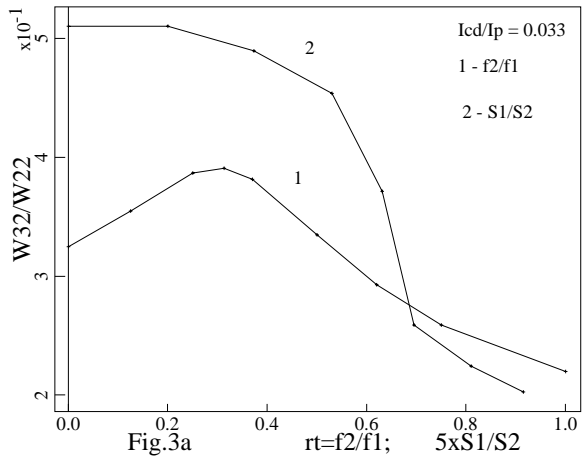
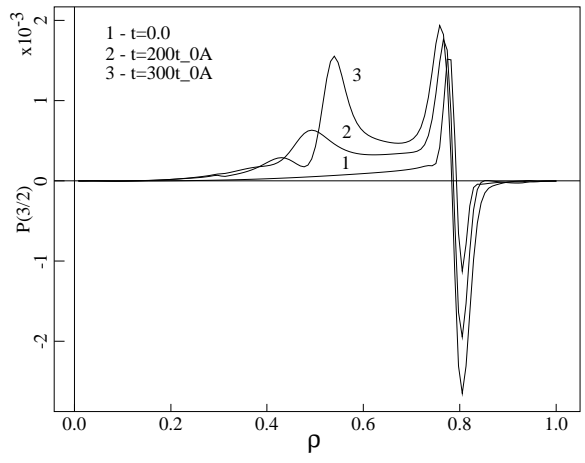


Fig.3a

Fig.3b Pressure  $P(3/2)$  in a sawtooth period.



Poincare map in sawtooth crash.  $q_{min}=0.985$ .

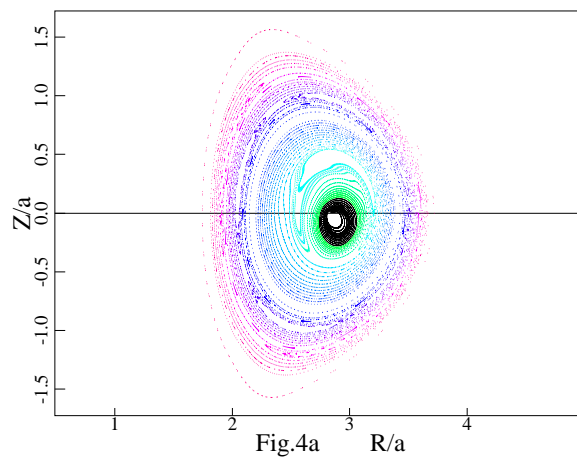


Fig.4a

Contour plot of pressure perturbation.

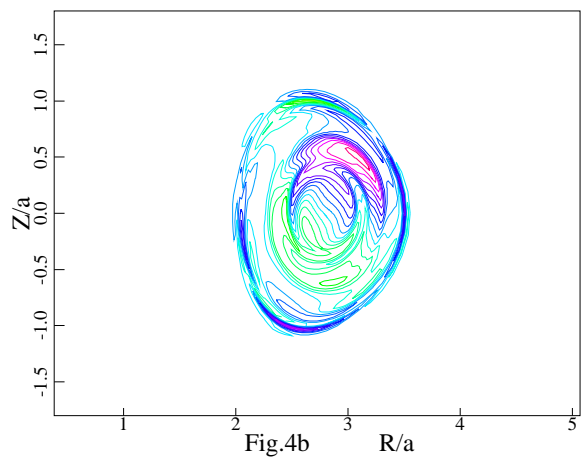


Fig.4b